

## **Improved Adhesion and Corrosion Resistance of an epoxy/Zn-5Al Composite Coating via NaF in a Phosphate Solution**

Ziwen Sun, Gang Kong, Yanqi Wang\*, Zhenping Chen, Chunshan Che

School of Materials Science and Engineering, South China University of Technology, Guangzhou 510640, China

\*E-mail: [sub\\_corrosion@163.com](mailto:sub_corrosion@163.com)

*Received:* 24 January 2019 / *Accepted:* 1 May 2019 / *Published:* 10 June 2019

---

The effect of NaF concentration on the formation of a phosphate film on a hot-dipped Zn-5Al coating, and consequently, the adhesion of the epoxy/Zn-5Al composite coating, has been investigated in this paper. The results showed that the morphology of the phosphate film and the adhesion, as measured by the tape test according to ASTM D3359, strongly depend on the concentration of the fluoride ions derived from NaF in the phosphate solution. Adhesion failure of an electrostatically sprayed epoxy on a bare hot-dipped Zn-5Al coating can be prevented with the optimal concentration of NaF (0.4 g/L) in a phosphate solution used in this study. At the same time, phosphating improved the corrosion resistance of the Zn-5Al coating in a NaCl solution.

---

**Keywords:** Fluoride; Phosphating; Adhesion; Epoxy /Zn-5Al duplex coating

### **1. INTRODUCTION**

The function of protective organic coatings is mainly to prevent the corrosion of metallic structures. Many studies [1-7] have focused on the corrosion resistance of epoxy coatings. These studies have shown that epoxy coatings obviously show a substantially superior performance against chloride-induced corrosion than that of other commercial coatings, such as red-oxide and zinc primer. Dong [3] investigated the corrosion behaviour of epoxy/zinc-coated rebar embedded in concrete in a marine environment. Galvanized coatings can provide effective protection when the epoxy coating is damaged, and epoxy coatings are helpful for ensuring galvanic protection of the galvanized coatings of steel. As an iron-zinc intermetallic phase exists in Zn coatings [8], when the epoxy/zinc composite-coated bar is bent during construction, cracking easily occurs in the Zn coating. Zn-Al coatings, which have excellent ductility [8,9] is a good alternative substrate for preventing cracking when an epoxy/Zn-

Al composite-coated bar is bent during construction. In practical applications, the epoxy resin of an epoxy/Zn-5Al composite coating can easily fall off.

Phosphating is often used to improve the adhesion of epoxy coatings to steel [11,12,13].  $\text{NaNO}_2$ , as an accelerator, plays an important role in steel passivation [10] and can directly affect the bonding force of an epoxy/metal composite coating. Zinc phosphating pre-treatment of metal surfaces is widely used to improve paint adhesion by providing a surface with numerous anchoring sites and to provide a barrier to prevent the spread of corrosion under the film [13]. The formation of a phosphate layer, which influences paint adhesion, depends on the phosphating parameters, such as temperature, phosphating time, fluoride ion concentration, alloy microstructure and metal ions [14-22]. The outer surface of a hot-dipped Zn-Al coating is mainly composed of  $\text{Al}_2\text{O}_3$  [23], which inhibits the deposition of phosphate crystals [22]. The presence of free fluoride results in a thinner oxide layer on the substrate, maintains the activity of the metallic surface and permits the nucleation and growth of the conversion coating [24,25]; however, studies on the influence of fluoride ions on paint adhesion are limited [14,19]. The aim of this paper is to research the influence of  $\text{F}^-$  from phosphating on the morphology of a Zn-5Al coating to obtain high paint adhesion for an epoxy-coated hot-dipped Zn-5Al coating. Additionally, the adhesion failure of the epoxy/Zn-5Al composite coating is discussed. Scanning electron microscope (SEM), electrochemical impedance spectroscopy (EIS), potentiodynamic polarization and adhesion, as measure by a tape test, are performed in this paper.

## 2. EXPERIMENTAL

### 2.1. Materials

Q235 cold-rolled steel sheets (40 mm×30 mm×0.8 mm) and Q235 steel bars ( $\text{Ø}$ =16 cm, length=100 cm) were chosen as the substrates for hot-dip galvanizing. A Zn-5Al alloy ingot was prepared using pure Zn (>99.995%) and pure Al (>99.90%). After pickling, washing, fluxing and drying, the steel sheet samples were hot-dip galvanized at 460°C for 1 min. A Zn-5Al coated bar was provided by Xiamen New Steel Company. The thickness of the Zn-5Al coating was ~40  $\mu\text{m}$ .

A phosphating solution, comprising ZnO (1.2 g/l),  $\text{NaNO}_3$  (15 g/l),  $\text{H}_3\text{PO}_4$  (15 ml/l), was used at pH=3.0, T=40°C for t=5 min, with different NaF concentrations (NaF=0, 0.2, 0.4, 0.6, 0.8 and 1.0 g/l) to investigate the influence of fluoride ions on the morphology of the phosphate film and the adhesion of the epoxy/Zn-5Al composite coating.

After phosphating, a low-temperature curing powder (3 M) was used for the epoxy/Zn-5Al composite coating.

### 2.2. Preparation of the epoxy/Zn-5Al composite coating

The hot-dipped Zn-5Al coating, as a substrate for epoxy spray coating, was heated in a chamber at ~250°C. Then, an epoxy coating process was followed with an operating voltage of 50 kV,

power pressure of 0.5 MPa, power amount of 100 g/min, spray distance of 100~150 mm, and spray thickness of ~180  $\mu\text{m}$  using an electrostatic spraying device (Spray-V26A).

### 2.3. Characterization methods

The adhesion of the epoxy/Zn-5Al duplex coating was measured by a tape test according to ASTM D3359.

The morphologies of the phosphate film and the epoxy inner surface at the adhesion failure points were characterized by scanning electron microscopy (SEM, Quanta 200), energy dispersive spectroscopy (EDS, Inca300) and X-ray diffraction (XRD, X'Pert Pro MRD). Potentiodynamic polarization and EIS measurements were carried out on hot-dipped Zn-5Al-coated sheet samples with and without phosphating in a 5% NaCl solution. Samples with an exposed area of 1  $\text{cm}^2$  in a 5% NaCl solution were used as the working electrode, platinum foil acted as the counter electrode and a KCl-saturated calomel electrode (SCE) acted as the reference electrode. EIS was measured over a frequency range from 100 kHz to 0.01 Hz. The potentiodynamic polarization curves were measured with a scan rate of 1 mV/s.

In addition, to simulate the field application of the composite coating, the epoxy/Zn-5Al-coated steel samples were bent into an arc with a diameter 4 times of the steel sample diameter, according to Chinese Standard GB/25826, to investigate the adhesion of the epoxy/Zn-5Al composite coating.

## 3. RESULTS AND DISCUSSION

### 3.1. Adhesion failure of the epoxy/Zn-5Al composite coating without phosphating

Fig. 1 shows the epoxy coating flaking that occurred when the epoxy/Zn-5Al composite-coated bars were bent into an arc with a diameter 4 times of the steel sample diameter. Only a small amount of tiny cracks appeared in the coatings of the bars stored under ambient conditions for one week (Fig. 1a), while obvious cracks could be visually observed in the coatings of the bars stored for 1 month (Fig. 1b), and the epoxy coating had obviously been peeled off when the bars were stored for 3 months. These results show that the adhesion of the epoxy coating on Zn-5Al decreased with increasing storage time. Fig. 2 shows that a large amount of a white substance, which was surrounded by numerous cracks, was dispersed on the inner surface of the peeled epoxy coating. EDS analysis indicated that the white substance consisted mainly of Zn, O and Fe. The white substance may be the corrosion products that form on the surface of the Zn-5Al coating.

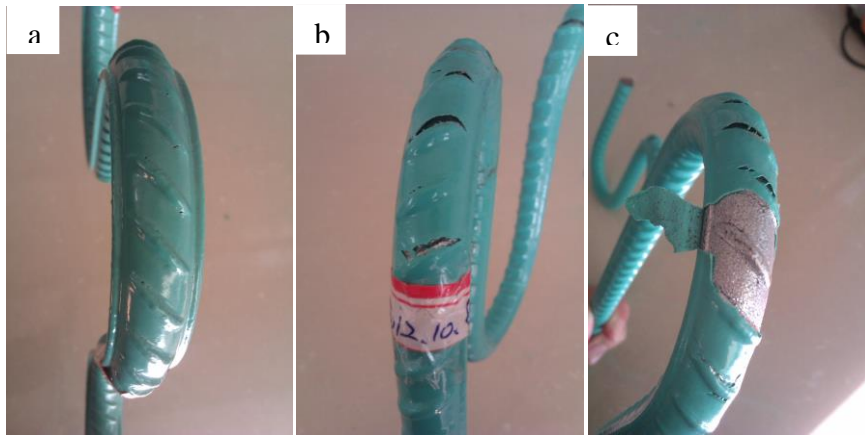


**Figure 1.** Bending test of epoxy-coated rebar after storing for (a) a week, (b) a month and (c) three months

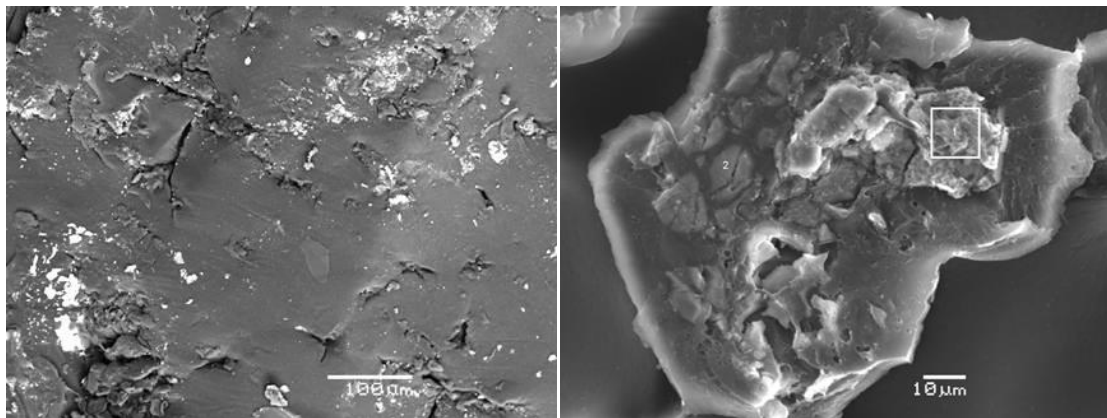


**Figure 2.** SEM images of the inner surface of the peeled epoxy

### 3.2. Phosphating

Fig. 3 shows SEM images of the phosphate film on the hot-dipped Zn-5Al coating prepared with phosphating solutions with different NaF concentrations. Preferential plate-like deposition of the phosphate products was observed on the samples treated with a phosphating solution without NaF, and several regions of the sample surface could not be coated with the phosphate film with obvious coarse plate-like crystals being observed instead (Fig. 3a). Needle-like phosphate products were observed to grow preferentially in a 0.2 g/L NaF solution, and the sizes of the phosphate platelets were more uniform (Fig. 3b). Fig. 3 shows that, with increasing concentration of NaF between 0-0.4 g/L, the size of the phosphate platelets decreased, and the surface coverage of the phosphate platelets increased. However, the opposite trend was observed when the NaF concentration was increased from 0.4 g/L to 1.0 g/L. Compared to phosphating without NaF (Fig. 3a), the surface coverage of the phosphate film with NaF increased, and needle-like platelets appeared. Among the different samples, the phosphate film with 0.4 g/L NaF had the highest coverage and the largest number of tiny needle-like phosphating platelets.

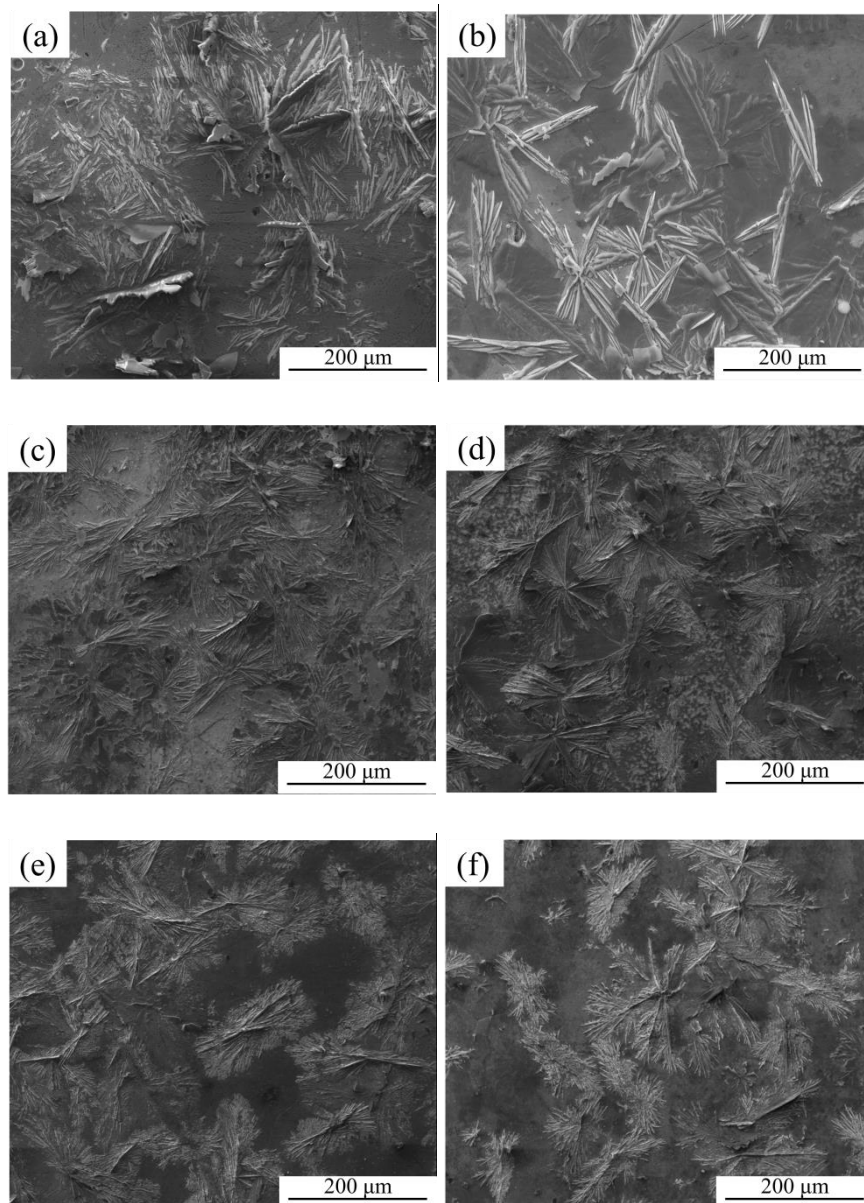


**Figure 3.** SEM images of the phosphate film treated with PS with NaF concentrations of (a) 0 g/L, (b) 0.2 g/L, (c) 0.4 g/L, (d) 0.6 g/L, (e) 0.8 g/L and (f) 1.0 g/L

The highest surface coverage of phosphate platelets and the smallest crystal size of the samples were obtained when treating with a phosphating solution containing 0.4 g/L NaF. To better understand the composition and growth orientation of the phosphate products. A high-magnification image of the phosphate film was obtained (Fig. 4). Fig. 4 shows that two different growth orientations of the phosphate products were observed: one growth orientation perpendicular to the substrate or at a certain inclination angle to the substrate, and the other growth orientation approximately parallel to the substrate. The different growth orientations facilitated the improvement of the paint adhesion by providing a surface with numerous anchoring points [8]. Needle-like platelets that grew at a certain inclination angle to the substrate were uniformly deposited onto the Zn-5Al coating with the addition of 0.4 g/L NaF to the phosphate solution.

The needle-like phosphate film, which was grown with two different orientations, is shown in Fig. 4. EDS analysis indicated that the phosphate film mainly consisted of Zn, P and O (shown in Table 1), which may imply that the phosphate film was mainly composed of  $Zn_3(PO_4)_2$ . However, Al was not detected by EDS analysis, and the amount of  $AlPO_4$  in the phosphate film, as proposed in a previous study [17], may be very small, or  $AlPO_4$  may not appear in the phosphate film. The X-ray diffraction pattern of the conversion coating on the Zn-5Al alloy is represented in Fig. 5. As shown in Fig. 5, Zn, ZnO and  $Zn_3(PO_4)_2$  diffraction peaks appeared, indicating that there was a phosphate-based film on the Zn-5Al coating after passivation.

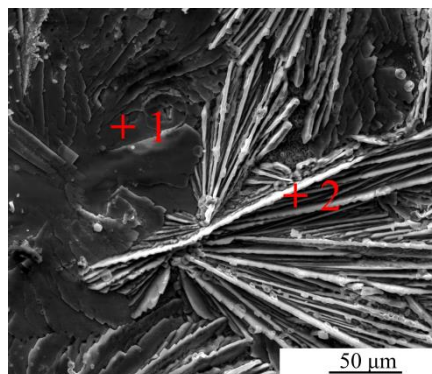


**Figure 4.** High-magnification SEM image of the phosphate film for sheet samples treated with a phosphating solution with 0.4 g/L NaF

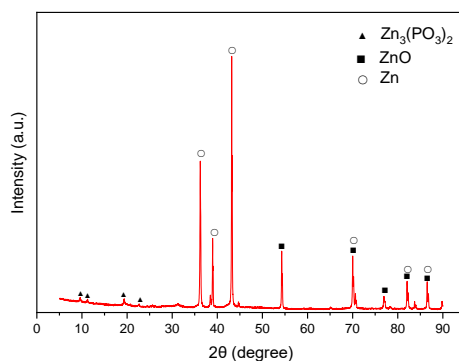


**Figure 5.** XRD pattern of the phosphate film formed on the Zn-5Al coating

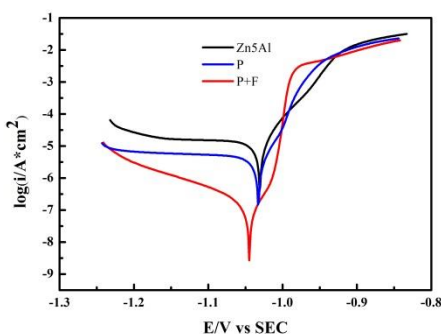
**Table 1.** Composition of the phosphate film from Fig. 4 (%)

Test point	Zn	P	O	P/O
1	23.6	10.7	65.7	0.163
2	19.1	11.3	69.6	0.162

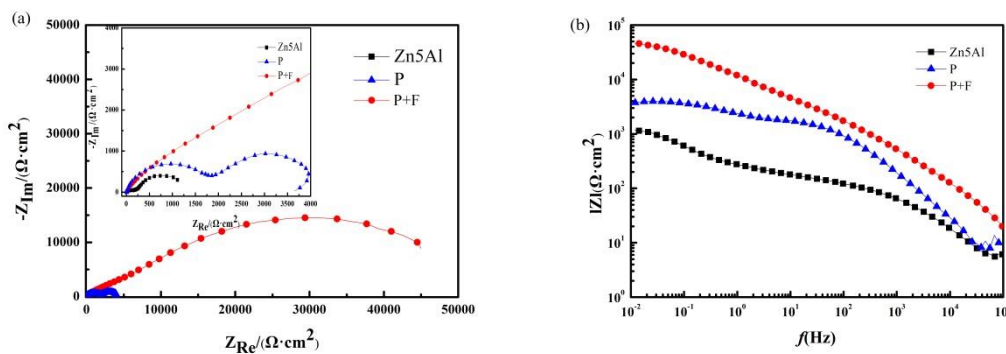
### 3.3. Electrochemical analysis

Fig. 6 shows the potentiodynamic polarization curves of the Zn-5Al coating treated with phosphating (0.4 g/L NaF, labelled P+F), phosphating without NaF (labelled P) and without phosphating (labelled Zn5Al) in a 5% NaCl solution. Fig. 6 shows that for the phosphate film, the

cathode and anode branches decreased compared to those of the Zn-5Al coating. The phosphate film curve shows a lower current density, which indicates that the corrosion products were less porous after pre-phosphating [28]. The corrosion currents  $I_{\text{corr}}$  of the polarization curves could be obtained by the Tafel extrapolation method, and the detailed parameters decreased from  $15 \mu\text{A}/\text{cm}^2$  to  $0.4 \mu\text{A}/\text{cm}^2$ . These results suggested that the corrosion rate of the phosphating film was lower than that of the Zn-5Al coating and that the corrosion rate of the phosphate film with  $0.4 \text{ g/L NaF}$  was lower than that of the phosphate film with no NaF. Compared to the Zn-5Al coating, the two phosphate films were conducive to improving the corrosion resistance. Therefore, it was found that the phosphate films distinctly possessed better corrosion resistance than that of the bare Zn-5Al coating. The phosphate film with NaF had better corrosion resistance than that of the phosphate film without NaF. Fig. 7 shows the EIS plots of the Zn-5Al coatings treated with phosphating (P and P+F) and without phosphating (Zn-5Al) obtained in a 5% NaCl solution. The capacitive impedance of the phosphate film prepared with  $0.4 \text{ g/L NaF}$  (P+F) was obviously larger than that of the phosphate film without NaF (P) and the Zn-5Al coating. The  $|Z|$  values of the Bode plots show that the impedance values increased after pre-phosphating. The formation of a dense phosphate film resulted in an increased impedance. The results obtained from the EIS measurements coincide well with the polarization curves.



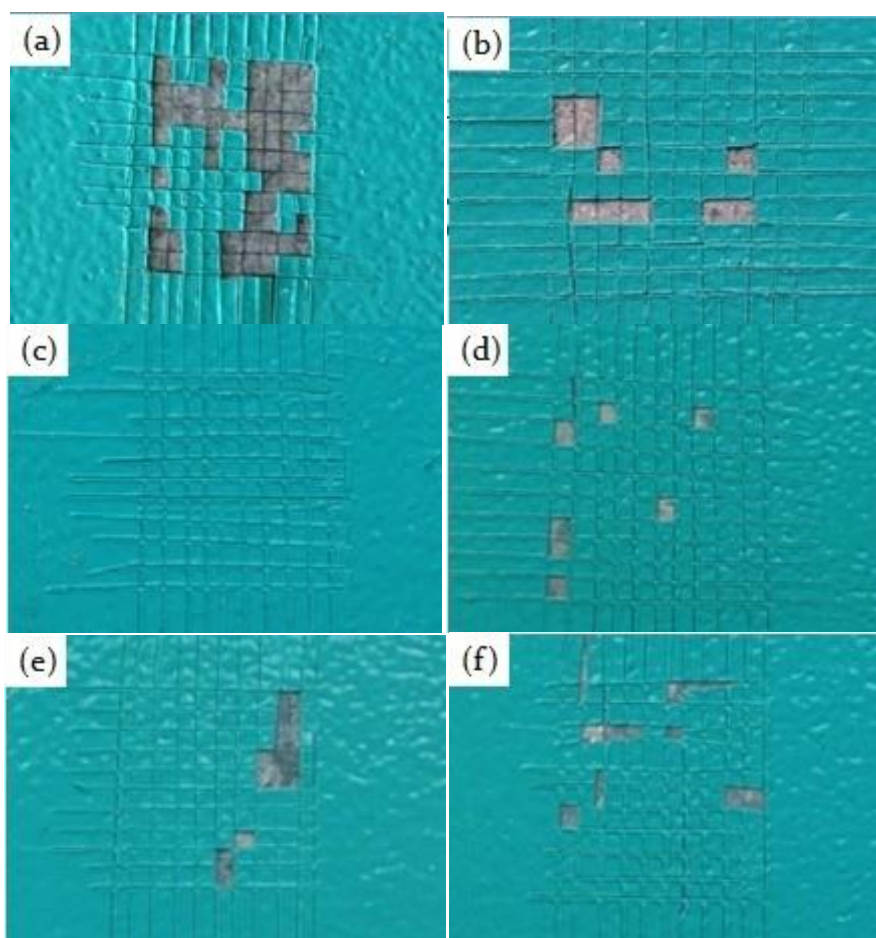
**Figure 6.** Potentiodynamic polarization curves obtained in 5%NaCl solution for the Zn-5Al coatings treated with phosphating and without phosphating



**Figure 7.** Nyquist plots (a) and Bode diagrams (b) obtained in 5% NaCl solution for the Zn-5Al coatings treated with phosphating with  $0.4 \text{ g/L NaF}$  (P+F), phosphating without NaF(P) and without phosphating (Zn5Al)

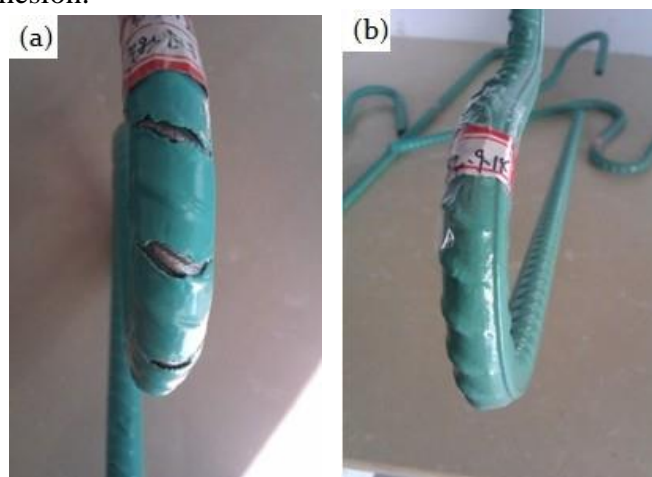
### 3.4. Adhesion measured by a tape test

Fig. 8 shows the results of the adhesion, as measured by a tape test according to ASTM D3359, of sheet samples treated with phosphating solutions with different NaF concentrations. Approximately 50% detachment was observed in the cross cuts for the phosphate-treated samples prepared without NaF. These samples showed the lowest adhesion among the different treatments, which could be because of the nonuniform growth of the phosphate platelets, which was bad for the adhesion of the epoxy to the substrate (Fig. 8a). The detachment rate decreased as the NaF concentration increased from 0 to 0.4 g/L; however, the opposite trend was observed as the NaF concentration was further increased from 0.4 g/L to 1.0 g/L, which was in agreement with the change in the morphologies of phosphate films observed in Fig. 3. Namely, the adhesion of the epoxy strongly depended on the morphology of the phosphate platelets and the surface coverage rate of the phosphate products, which provide numerous anchoring points and are dependent on the NaF concentration in the phosphating solution. A NaF concentration of approximately 0.4 g/L was the optimal concentration in the phosphating solutions used in this study.



**Figure 8.** Influence of the NaF concentration on the coating adhesion: (a) 0 g/L, (b) 0.2 g/L, (c) 0.4 g/L, (d) 0.6 g/L, (e) 0.8 g/L and (f) 1.0 g/L

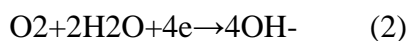
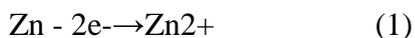
To verify the high adhesion force of the epoxy/composite coating treated with a phosphating solution with 0.4 g/L NaF. A bending test was carried out using epoxy-coated bar samples (details in section 2.1) treated with a phosphating solution containing 0.4 g/L NaF for 3 months. Fig. 9 shows that the adhesion of the pre-phosphating bar samples was improved, and no evident cracking could be observed compared to that of bar samples without pre-phosphating when the samples were bent into an arc with a diameter of 4 times of the sample diameter. The test results showed that it is necessary to treat hot-dipped Zn-Al coatings by phosphating with a proper NaF concentration before epoxy-coating to improve the coating adhesion.



**Figure 9.** Bending test of the composite-coated bar samples after 3 months with different treatments: (a) without phosphating and (b) phosphating with 0.4 g/L NaF

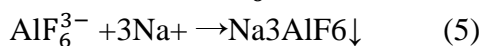
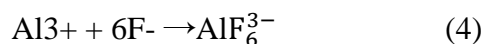
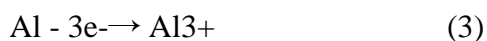
### 3.5. Discussion

The epoxy coating was destroyed when the epoxy/Zn-5Al composite-coated bars were bent into an arc after being stored for a long period of time. A large amount of a white substance, which was the corrosion products of the Zn-5Al coating, was dispersed on the inner surface of the peeled epoxy. EDS analysis showed that the white substance consisted mainly of Zn, O and Fe. It was most likely that the Fe-Zn intermetallic, which was attached to the Zn-5Al coating during the galvanizing process, acted as a defect in the epoxy/Zn-5Al composite coating and was dissolved as the anode in reaction (1) to form the corrosion products, which may promote epoxy delamination [26]. The cathodic reaction (2) also occurred between the epoxy and oxidation layer. The high alkalinity at the cathode may favour the dissolution of the oxidation layer and promote delamination to form a weak adhesion zone (the zone with cracks in Fig. 2). The application of a mechanical load during the bending process of the epoxy-coated bars resulted in the removal of materials in zones with weak adhesion [22,26].



Phosphating was used to improve the adhesion of the epoxy/Zn-5Al coating. Because of the appearance of  $\text{Al}_2\text{O}_3$  on the outer surface of the Zn-5Al coating [23,28], passivation could have been hindered when the hot-dipped Zn-5Al coating was immersed into the phosphating solution. For the

aluminium in the Zn-Al coating, the addition of free fluoride ions to the phosphating solution was necessary to produce a thinner oxide layer on the metallic substrate (reactions (3) and (4)), to control the amount of aluminium in solution (reaction (5)), to maintain the surface activity and to achieve a proper coating [14,24]. The uniform growth of the phosphate platelets was promoted when the NaF concentration was increased from 0.2 g/L to 0.4 g/L, and the coverage rate also improved (Fig. 3a, Fig. 3b and Fig. 3c). Under certain circumstances, NaF promoted phosphate film formation. Then the NaF concentration was greater than 0.6 g/L, the film was difficult to grow and was incomplete. This may be due to the differences in the standard potentials of zinc ( $-0.76$  V) and aluminium ( $-1.66$  V); thus, Al on the Zn-Al alloy surface dissolved in the phosphating solution to generate electrons, which reduced some of the  $Zn^{2+}$  near the surface into metallic Zn deposited onto the surface at the micro cathodic sites and became part of the composition of the phosphate coating [27]. The Al dissolution rate rapidly increased as the NaF concentration increased (Fig. 3d, Fig. 3e and Fig. 3f). Reaction (6) may deposit metallic Zn onto the surface, which may hinder the growth of phosphate platelets and lower the degree of surface coverage.



The phosphate film has two different orientations. The different growth orientations facilitated paint adhesion by providing a surface with numerous anchoring points [13]. The phosphate coating with 0.4 g/L NaF had a more perpendicular structure and relatively more anchoring points than those of the other coatings, thus promoting epoxy adhesion.

#### 4. CONCLUSION

In this work, an attempt was made to improve the adhesion of an epoxy/Zn-5Al composite coating. The morphology of the phosphate film and paint adhesion strongly depended on the NaF concentration in the phosphate solution used in this study. The test results showed that for an epoxy/Zn-5Al-coated rebar without phosphating, obvious cracks appeared when a bending test was performed; however, no obvious cracks were observed for the epoxy/Zn-5Al-coated rebar with the optimal phosphate coating. Phosphating passivation with the addition of NaF improved the adhesion and corrosion resistance of the epoxy/Zn-5Al coating.

#### References

1. F. Tang, B. Yi, Y. Chen, Y. Tang, G. Chen, *Constr. Build. Mater.*, 112(2016) 7.
2. M.M.H. Al-Tholaia, A.K. Azad, S. Ahmad, M.H. Baluch, *Constr. Build. Mater.*, 56 (2014) 74.
3. S.G. Dong, B. Zhao, C.J. Lin, R.G. Du, R.G. Hu, G.X. Zhang, *Constr. Build. Mater.*, 28 (2012) 72.
4. S. González, M.A. Gil, J.O. Hernández, V. Fox, R.M. Souto, *Prog. Org. Coat.*, 41 (2001) 167.
5. J.B. Bajat, Z. Kacarević, V.B. Mišković-Stanković, M.D. Maksimović, *Prog. Org. Coat.*, 39 (2000) 127.

6. Ş. Erdoğdu, T.W. Bremner, I.L. Kondratova, *Cem. Concr. Res.*, 31 (2001) 861.
7. H.Z. Lo'pez-Calvo, P. Montes-Garcia, I. Kondratova, T.W. Bremner and M.D.A. Thomas, *Mater. Corros.*, 64(2013) 599.
8. A.R. Marder, *Prog. Mater. Sci.*, 45 (2000) 191.
9. Z.W. Sun, G. Kong, C.S. Che, Y.Q. Wang, X.R. Miao, *Surf. Interface Anal.*, 56 (2019) 465.
10. B.V. Jegdić, J.B. Bajat, J.P. Popić, S.I. Stevanović, V.B. Mišković-Stanković, *Corros. Sci.*, 53 (2011) 2872.
11. B. Ramezanzadeh, H. Vakili, R. Amini, *Appl. Surf. Sci.*, 327 (2015) 174.
12. H. Vakili, B. Ramezanzadeh, R. Amini, *Corros. Sci.*, 94 (2015) 466.
13. S. Jegannathan, T.S.N.S. Narayanan, K. Ravichandran, S. Rajeswari, *Surf. Coat. Technol.*, 200 (2006) 6014.
14. V. Burokas, A. Martušienė, O. Girčienė, *Surf. Coat. Technol.*, 202 (2007) 239.
15. G. Bustamante, F.J. Fabri-Miranda, I.C.P. Margarit, O.R. Mattos, *Prog. Org. Coat.*, 46 (2003) 84.
16. C.Y. Tsai, J.S. Liu, P.L. Chen, C.S. Lin, *Corros. Sci.*, 52 (2010) 3907.
17. D. Susac, X. Sun, R.Y. Li, K.C. Wong, P.C. Wong, K.A.R. Mitchell, R. Champaneria, *Appl. Surf. Sci.*, 239 (2004) 45.
18. N.V. Phuong, S. Moon, D. Chang, K.H. Lee, *Appl. Surf. Sci.*, 264 (2013) 70.
19. J.B. Bajat, V.B. Mišković-Stanković, J.P. Popić, D.M. Dražić, *Prog. Org. Coat.*, 63 (2008) 201.
20. S. Palraj, M. Selvaraj, P. Jayakrishnan, *Prog. Org. Coat.*, 54 (2005) 5.
21. N. Rezaee, M.M. Attar, B. Ramezanzadeh, *Surf. Coat. Technol.*, 236 (2013) 361.
22. S. Maeda, *Prog. Org. Coat.*, 28 (1996) 227.
23. S. Feliu Jr., V. Barranco, *Acta Mater.*, 51 (2003) 5413.
24. O. Lunder, J.C. Walmsley, P. Mack, K. Nisancioglu, *Corros. Sci.*, 47 (2005) 1604.
25. M.F. Abd Rabbo, J.A. Richardson, G.C. Wood, *Corros. Sci.*, 18 (1978) 117.
26. N.F. Garza-Montes-de-Oca, R. Colas, *Eng. Failure Anal.*, 26 (2012) 175.
27. G.Y. Li, J.S. Lian, L.Y. Niu, Z.H. Jiang, Q. Jiang, *Surf. Coat. Technol.*, 201 (2006) 1814.
28. Z.J. Cao, G. Kong, C.S. Che, Y.Q. Wang, *Appl. Surf. Sci.*, 426 (2017) 67.

© 2019 The Authors. Published by ESG ([www.electrochemsci.org](http://www.electrochemsci.org)). This article is an open access article distributed under the terms and conditions of the Creative Commons Attribution license (<http://creativecommons.org/licenses/by/4.0/>).